

An Improved Search Method for Gravitational Ringing of Black Holes

Hiroyuki Nakano¹, Hirotaka Takahashi^{2,3,4}, Hideyuki Tagoshi^{3,5} and Misao Sasaki⁴

¹*Department of Mathematics and Physics, Graduate School of Science, Osaka City University,
Osaka 558-8585, Japan*

²*Department of Physics, Graduate School of Science and Technology, Niigata University,
Niigata 950-2181, Japan*

³*Department of Earth and Space Science, Graduate School of Science, Osaka University,
Toyonaka, 560-0043, Japan*

⁴*Yukawa Institute for Theoretical Physics, Kyoto University,
Kyoto 606-8502, Japan*

⁵*Theoretical Astrophysics, California Institute of Technology, Pasadena, CA 91125, USA*

February 18, 2022

A black hole has characteristic quasi-normal modes that will be excited when it is formed or when the geometry is perturbed. The state of a black hole when the quasi-normal modes are excited is called the gravitational ringing, and detections of it will be a direct confirmation of the existence of black holes. To detect it, a method based on matched filtering needs to be developed. Generically, matched filtering requires a large number of templates, because one has to ensure a proper match of a real gravitational wave with one of template waveforms to keep the detection efficiency as high as possible. On the other hand, the number of templates must be kept as small as possible under limited computational costs. In our previous paper, assuming that the gravitational ringing is dominated by the least-damped (fundamental) mode with the least imaginary part of frequency, we constructed an efficient method for tiling the template space. However, the dependence of the template space metric on the initial phase of a wave was not taken into account. This dependence arises because of an unavoidable mismatch between the parameters of a signal waveform and those given discretely in the template space. In this paper, we properly take this dependence into account and present an improved, efficient search method for gravitational ringing of black holes.

I. INTRODUCTION

Thanks to the recent technological advance, there are many on-going projects of gravitational wave detection in the world; the Laser Interferometric Gravitational Wave Observatory (LIGO) [1], VIRGO [2], GEO-600 [3], ACIGA [4], TAMA300 [5] and the Large-scale Cryogenic Gravitational wave Telescope (LCGT) [6] which are ground-based laser interferometers, and EXPLORER [7], ALLEGRO [8], NIOBE [9], NAUTILUS [10] and AURIGA [11] which are bar detectors. Furthermore, there are some future space interferometer projects such as the Laser Interferometer Space Antenna (LISA) [12] and the DECi hertz Interferometer Gravitational wave Observatory (DECIGO) [13]. The detection of gravitational waves provides us with not only a direct experimental test of general relativity but also a new window to observe our Universe. To use them as a new tool of observation, it is necessary to derive theoretical waveforms. Once we know them, we may appeal to the matched filtering technique to extract source's information from gravitational wave signals. However, because the signals are expected to be very weak and the amount of data will be enormous for long-term continuous observations, it is essentially important to develop efficient data analysis methods.

For these ground-based as well as future space-based interferometers, coalescence of compact object binaries is the most important source of gravitational waves. The process of a binary coalescence can be divided into three distinct phases. During the initial *inspiral* phase, the gravitational radiation reaction timescale is much longer than the orbital period. The gravitational waves from the inspiral phase carry the information of the masses, spins and so on, of the system. After the inspiral phase, the binary becomes dynamically unstable and starts to merge. This phase is called the *merger* phase. The gravitational waves from the merger phase give us the information about fully general relativistic dynamics of the system. Finally, if a black hole is formed after the merger phase, the system enters the *ringdown* phase where it gradually settles down to a stationary Kerr black hole. During this process, the black hole

emits gravitational waves with frequencies and damping rates specific to its mass and spin. Thus, the gravitational waves in the ringdown phase carry the information of the mass and spin of the final black hole.

In this paper, we consider an effective search method for gravitational ringing of distorted spinning (Kerr) black holes. The ringdown waves are described by quasi-normal modes of a black hole. The quasi-normal modes are complex frequency wave solutions of the perturbed Einstein equations with purely outgoing-wave boundary condition at infinity and ingoing-wave at horizon, with vanishing incoming-wave amplitude. A quasi-normal mode is characterized by the central frequency f_c , usually called the (quasi-)normal-mode frequency, and the quality factor Q which is inversely proportional to the imaginary part of the complex frequency. Their properties were analyzed extensively by Leaver [14], and it is known that the least-damped (fundamental) mode belongs to the $\ell = m = 2$ spin-2 spheroidal harmonic modes. We note that a ringdown signal decays exponentially. Therefore, unless the signal-to-noise ratio (SNR) is very large, the signal will be soon buried in the noise after a few oscillation cycles. So, it is essentially important to keep the loss of SNR as small as possible when we construct a search method.

Here we consider a black hole characterized by its mass M and the dimensionless spin parameter $a = J/M^2$ where J is the spin angular momentum. The parameter a takes a value in the range $[0, 1]$, with $a = 0$ corresponding to a Schwarzschild black hole and $a = 1$ to an extreme Kerr black hole. It is known that the imaginary part of the $\ell = m = 2$ least-damped mode is the smallest of all the quasi-normal modes, and results of black hole perturbation calculations as well as numerical relativity simulations strongly suggest that a ringdown wave is dominated by this $\ell = m = 2$ least-damped mode unless a is extremely close to unity. Hence we focus on this single mode. Then a ringdown waveform is expressed as

$$h(f_c, Q, t_0, \phi_0; t) = \begin{cases} e^{-\frac{\pi f_c (t-t_0)}{Q}} \cos(2\pi f_c (t-t_0) - \phi_0) & \text{for } t \geq t_0, \\ 0 & \text{for } t < t_0, \end{cases} \quad (1.1)$$

where we set the amplitude to unity for simplicity, and t_0 and ϕ_0 are the initial time and phase of the ringdown wave, respectively. For the $\ell = m = 2$ least-damped mode, analytical fitting formulas for the central frequency f_c and quality factor Q were given by Echeverria [15] as

$$f_c \simeq 32\text{kHz} [1 - 0.63(1-a)^{0.3}] \left(\frac{M}{M_\odot}\right)^{-1}, \quad (1.2)$$

$$Q \simeq 2.0(1-a)^{-0.45}. \quad (1.3)$$

There exists rich literature on search methods for ringdown waves. Echeverria [15] investigated the problem of extracting the black hole parameters from gravitational wave data in the case when SNR is large. Finn [16] improved this situation by developing a maximum likelihood analysis method that can deal with any SNR. Flanagan and Hughes then considered the parameter extraction from the three stages of a binary coalescence, i.e., from inspiral, merger and ringdown phases, in their series of papers [17]. For the ringdown phase, they discussed the relation between the energy spectrum of the radiation and SNR. Creighton [18] reported the result of analyzing data of the Caltech 40m by matched filtering, and emphasized the importance of coincidence event searches to discriminate spurious events from real events. But the search was limited to a single ringdown wave template. Recently, Arnaud et al. [19] discussed a tiling method to cover the 2-dimensional template space $\{f_c, Q\}$. In our previous paper [20], we proposed a more efficient method for tiling the template space. There, however, we ignored the dependence of the metric of the template space $\{f_c, Q\}$ on the initial phase ϕ_0 . This induces some small but non-negligible decrease in the match for a signal with certain ranges of ϕ_0 . In this paper, we remove this shortcoming by properly taking into account the initial phase dependence, and develop a similar but substantially improved template spacing which is much more reliable than the previous one.

Here we make a comment on an analysis using real interferometers' data. In this case, we have to deal with non-stationary, non-Gaussian noises, and Tsunesada and Kanda [21] found that more fake events are observed than in the case of an inspiraling wave search, because the duration of a ringdown wave is typically much shorter than that of an inspiral wave and it can easily be affected by short bursts. It will be necessary to develop a way to remove such fake events without losing real ringdown signals, but we leave this issue for future work.

The paper is organized as follows. In Sec. II, first, we introduce orthonormal template waveforms for ringdown waves. Second, assuming a white noise background, we consider matched filtering in the 4-dimensional template space $\{t_0, \phi_0, f_c, Q\}$. We show that we can effectively reduce the template space to 2-dimensions spanned by $\{f_c, Q\}$, but the metric of this reduced template space depends on ϕ_0 . Then, by carefully taking account of the ϕ_0 dependence of the metric, we analytically develop an efficient and reliable tiling method for ringdown wave searches. In Sec. III, by using a fitting curve for the TAMA noise spectrum during the Data Taking 8 (DT8) in 2003, we show that our template spacing developed for white noise is valid even in the case of colored noise. Finally, Sec. IV is devoted to summary and discussion. In Appendix A, we recapitulate the tiling method we proposed in [20]. In Appendix B, we summarize the parameter estimation errors for ringdown signals by using the Fisher information matrix.

II. TEMPLATE SPACE

In this section, we present an improved version of the template spacing we have developed in our previous paper [20], which can be used for matched filtering of the quasi-normal ringing waveforms. Here, the detector noise is assumed to be white noise to make it possible to deal with the problem analytically.

A. Maximization over the initial phase ϕ_0

We have temporarily set the amplitude to unity for simplicity in Eq. (1.1). Note that the knowledge of the amplitude is not necessary for the template spacing in matched filtering. For $t \geq t_0$, the ringdown wave (1.1) is divided into two parts.

$$h(f_c, Q, t_0, \phi_0; t) = h_c(f_c, Q, t_0; t) \cos \phi_0 + h_s(f_c, Q, t_0; t) \sin \phi_0, \quad (2.1)$$

where

$$h_c(f_c, Q, t_0; t) = e^{-\frac{\pi f_c (t-t_0)}{Q}} \cos(2\pi f_c (t-t_0)), \quad (2.2)$$

$$h_s(f_c, Q, t_0; t) = e^{-\frac{\pi f_c (t-t_0)}{Q}} \sin(2\pi f_c (t-t_0)). \quad (2.3)$$

Performing the Fourier transformation $\tilde{h}_\sigma(f) = \int_{-\infty}^{\infty} dt e^{2\pi i f t} h_\sigma(t)$, where $\sigma = c$ or s , we obtain the waveforms in the frequency domain as

$$\tilde{h}_c(f_c, Q, t_0; f) = \frac{(f_c - 2i f Q) Q e^{2i\pi f t_0}}{\pi(2f_c Q - i f_c - 2f Q)(2f_c Q + i f_c + 2f Q)}, \quad (2.4)$$

$$\tilde{h}_s(f_c, Q, t_0; f) = \frac{2f_c Q^2 e^{2i\pi f t_0}}{\pi(2f_c Q - i f_c - 2f Q)(2f_c Q + i f_c + 2f Q)}. \quad (2.5)$$

The waveform in the time domain is real, so the following relation is satisfied.

$$\tilde{h}^*(f) = \tilde{h}(-f), \quad (2.6)$$

where the star (*) denotes the complex conjugation.

Here, we introduce the inner product as

$$(a, b) = 2 \int_{-f_{\max}}^{f_{\max}} df \frac{\tilde{a}(f) \tilde{b}^*(f)}{S_n(|f|)}, \quad (2.7)$$

where S_n is defined as a one-sided power spectrum density, and f_{\max} is the maximum frequency we take into account in the analysis. In the actual data analysis, it is equal to or less than the half of the sampling frequency of data. In this section, the detector noise is assumed to be white noise $S_n(|f|) = 1$. We will use the fitting curve for the TAMA DT8 noise spectrum as a colored noise in the next section.

In the matched filtering, we calculate the inner product between the template h and a signal x defined by (x, h) . First, we normalize the templates h_c and h_s . We define the normalization constants as

$$\begin{aligned} N_c(f_c, Q, t_0) &= (h_c(f_c, Q, t_0), h_c(f_c, Q, t_0)) \\ &= \frac{(2Q^2 + 1)Q}{\pi(4Q^2 + 1)f_c}, \end{aligned} \quad (2.8)$$

$$\begin{aligned} N_s(f_c, Q, t_0) &= (h_s(f_c, Q, t_0), h_s(f_c, Q, t_0)) \\ &= \frac{2Q^3}{\pi(4Q^2 + 1)f_c}, \end{aligned} \quad (2.9)$$

when we have set $f_{\max} = \infty$. It is noted that the normalization constant N_σ does not depend on the initial time. The normalized templates $\hat{h}_\sigma(f_c, Q, t_0)$ are given by

$$\hat{h}_\sigma(f_c, Q, t_0; f) = \frac{1}{\sqrt{N_\sigma(f_c, Q, t_0)}} \tilde{h}_\sigma(f_c, Q, t_0; f). \quad (2.10)$$

We note that the two parts, h_c and h_s , are not orthogonal. Their inner product is obtained as

$$\begin{aligned} (\hat{h}_c(f_c, Q, t_0), \hat{h}_s(f_c, Q, t_0)) &= \frac{1}{\sqrt{2(2Q^2 + 1)}} \\ &=: c(f_c, Q, t_0). \end{aligned} \quad (2.11)$$

Then the normalized ringdown template for the waveform (1.1) is given in the frequency domain as

$$\tilde{h}(\phi_0; f_c, Q, t_0; f) = \frac{1}{\sqrt{N(\phi_0; f_c, Q, t_0)}} \tilde{h}(f_c, Q, t_0, \phi_0; f), \quad (2.12)$$

where

$$\begin{aligned} \tilde{h}(f_c, Q, t_0, \phi_0; f) &= \frac{(\cos \phi_0 f_c - 2i \cos \phi_0 f Q + 2f_c Q \sin \phi_0) Q e^{2i\pi f t_0}}{\pi (2f_c Q - i f_c - 2f Q) (2f_c Q + i f_c + 2f Q)}, \\ N(\phi_0; f_c, Q, t_0) &= (h(f_c, Q, t_0, \phi_0), h(f_c, Q, t_0, \phi_0)) \\ &= N_c(f_c, Q, t_0) \cos^2 \phi_0 + N_s(f_c, Q, t_0) \sin^2 \phi_0 \\ &\quad + 2c(f_c, Q, t_0) \sqrt{N_c(f_c, Q, t_0) N_s(f_c, Q, t_0)} \cos \phi_0 \sin \phi_0. \end{aligned} \quad (2.13)$$

In an actual data analysis, instead of the normalized templates \hat{h}_c and \hat{h}_s , it is more convenient to prepare a set of orthonormalized waveforms h_1 and h_2 as templates. They can be obtained by Schmidt's orthonormalization. First, we choose

$$h_1(f_c, Q, t_0) = \hat{h}_c(f_c, Q, t_0). \quad (2.14)$$

Then the normalized waveform h_2 orthogonal to h_1 is obtained as

$$h_2(f_c, Q, t_0) = \frac{\hat{h}_s(f_c, Q, t_0) - c(f_c, Q, t_0) \hat{h}_c(f_c, Q, t_0)}{\sqrt{1 - c(f_c, Q, t_0)^2}}. \quad (2.15)$$

Using the above orthonormal templates, the SNR maximized over the initial phase ϕ_0 is given as

$$\rho(x; f_c, Q, t_0) = \max_{\phi_0} \left\{ \sqrt{(x, \hat{h}(f_c, Q, t_0, \phi_0))^2} \right\} = \sqrt{(x, h_1(f_c, Q, t_0))^2 + (x, h_2(f_c, Q, t_0))^2}, \quad (2.16)$$

where x represents a signal. We note that there is basically nothing wrong with using the non-orthogonalized templates \hat{h}_σ in the matched filtering. In the case we use the non-orthogonal templates, the maximization of (x, \hat{h}) over the phase ϕ_0 has been discussed by Mohanty [22], and the result is the same if we replace h_1 and h_2 in Eq. (2.16) by those given in Eqs. (2.14) and (2.15), respectively.

Before closing this subsection, let us describe how to determine the initial phase ϕ_0 from the filtered output. For simplicity, we take the normalized wave \hat{h} as a signal, because the overall amplitude is irrelevant for the present discussion. We further assume that there is a perfect match of the parameters $\{f_c, Q, t_0\}$ between the signal and a template, and the SNR is maximized, that is, $\rho(\hat{h}; f_c, Q, t_0) = 1$.

We consider the quantities,

$$\begin{aligned} \rho_1 &= (\hat{h}, h_1), \\ \rho_2 &= (\hat{h}, h_2). \end{aligned} \quad (2.17)$$

When the signal perfectly matches with a template, these are formally expressed as

$$\rho_1 = \frac{1}{\sqrt{N(\phi_0; f_c, Q, t_0)}} \left(\sqrt{N_c(f_c, Q, t_0)} \cos \phi_0 + c(f_c, Q, t_0) \sqrt{N_s(f_c, Q, t_0)} \sin \phi_0 \right) \quad (2.18)$$

$$\rho_2 = \frac{1}{\sqrt{N(\phi_0; f_c, Q, t_0)}} \sqrt{(1 - c(f_c, Q, t_0)^2) N_s(f_c, Q, t_0)} \sin \phi_0. \quad (2.19)$$

Taking the ratio of ρ_1 and ρ_2 , we find

$$\frac{\rho_1}{\rho_2} = \sqrt{\frac{N_c(f_c, Q, t_0)}{(1 - c(f_c, Q, t_0)^2) N_s(f_c, Q, t_0)}} \cot \phi_0 + \sqrt{\frac{c(f_c, Q, t_0)}{1 - c(f_c, Q, t_0)^2}}. \quad (2.20)$$

Thus, the initial phase of a ringdown wave signal is determined as

$$\phi_0 = \cot^{-1} \left[\sqrt{\frac{(1 - c(f_c, Q, t_0)^2) N_s(f_c, Q, t_0)}{N_c(f_c, Q, t_0)}} \frac{\rho_1}{\rho_2} - \sqrt{\frac{c(f_c, Q, t_0) N_s(f_c, Q, t_0)}{N_c(f_c, Q, t_0)}} \right]. \quad (2.21)$$

It is noted that $\phi_0 \sim \cot^{-1}(\rho_1/\rho_2)$ for large Q .

B. 3-dimensional distance function

In the previous subsection, we obtained the expression for the SNR maximized over the initial phase ϕ_0 , Eq. (2.16). Here, we consider the remaining 3 parameters $\{f_c, Q, t_0\}$, and derive the metric in the 3-dimensional template space that describes the degree of mismatch between a signal and a template. To this end, we point out an important fact that was overlooked in [20]. Given a signal with certain values of the parameters, the SNR defined by Eq. (2.16) will be independent of ϕ_0 for a template that matches exactly with the signal. However, it will not be so if there is no exact matching between the signal and a template. In other words, if there is a mismatch between the parameters of a signal and those of a template, the resulting SNR will depend on the initial phase ϕ_0 .

Let us define the match $C(\phi_0; df_c, dQ, dt_0)$ between the template with the parameters (f_c, Q, t_0, ϕ_0) and the normalized signal having slightly different values of the parameters $(f_c + df_c, Q + dQ, t_0 + dt_0, \phi_0)$. Note that, since we have already maximized the SNR over the initial phase ϕ_0 , it is unnecessary to consider the difference $d\phi_0$ for the match. The match $C(\phi_0; df_c, dQ, dt_0)$ is defined by

$$\begin{aligned} C(\phi_0; df_c, dQ, dt_0) &:= \rho \left(\hat{h}(f_c + df_c, Q + dQ, t_0 + dt_0, \phi_0); f_c, Q, t_0 \right) \\ &= \left[\sum_{A=1}^2 \frac{(h(f_c + df_c, Q + dQ, t_0 + dt_0, \phi_0), h_A(f_c, Q, t_0))^2}{(h(f_c + df_c, Q + dQ, t_0 + dt_0, \phi_0), h(f_c + df_c, Q + dQ, t_0 + dt_0, \phi_0))} \right]^{1/2} \\ &= 1 - \frac{1}{2(h(f_c, Q, t_0, \phi_0), h(f_c, Q, t_0, \phi_0))} \left[(h_{,i}(f_c, Q, t_0, \phi_0), h_{,j}(f_c, Q, t_0, \phi_0)) \right. \\ &\quad \left. - \sum_{A=1}^2 (h_{,i}(f_c, Q, t_0, \phi_0), h_A(f_c, Q, t_0)) (h_{,j}(f_c, Q, t_0, \phi_0), h_A(f_c, Q, t_0)) \right] dx^i dx^j \\ &\quad + O(dx^3) \\ &= 1 - ds_{(3)}^2 + O(dx^3), \end{aligned} \quad (2.22)$$

where $\{x^i\} = \{t_0, f_c, Q\}$ ($i = 1, 2, 3$), the comma $(,)$ denotes the partial differentiation, and we have introduced the 3-dimensional distance function in the template space by $ds_{(3)}^2 = 1 - C$. The smaller the match C is, the larger the distance is between the two signals in the template space.

If we introduce the metric [23] as

$$ds_{(3)}^2 = g_{ij}^{(3)} dx^i dx^j, \quad (2.23)$$

the components of the metric are explicitly written as

$$\begin{aligned} g_{t_0 t_0}^{(3)} &= \frac{4 \pi f_c f_{\max} (4 Q^2 + 1) \cos^2(\phi_0)}{Q (4 Q^2 + 2 Q \sin(2 \phi_0) + 1 + \cos(2 \phi_0))}, \\ g_{t_0 f_c}^{(3)} &= g_{f_c t_0}^{(3)} \\ &= \frac{\pi (4 Q^2 + 1) \sin(2 \phi_0)}{2 (4 Q^2 + 2 Q \sin(2 \phi_0) + 1 + \cos(2 \phi_0))}, \\ g_{t_0 Q}^{(3)} &= g_{Q t_0}^{(3)} \\ &= \frac{\pi f_c \cos(\phi_0) (2 Q \cos(\phi_0) - \sin(\phi_0))}{Q (4 Q^2 + 2 Q \sin(2 \phi_0) + 1 + \cos(2 \phi_0))}, \\ g_{f_c f_c}^{(3)} &= \frac{Q^2 (4 Q^2 - 2 Q \sin(2 \phi_0) + 1 - \cos(2 \phi_0))}{2 f_c^2 (4 Q^2 + 2 Q \sin(2 \phi_0) + 1 + \cos(2 \phi_0))}, \end{aligned}$$

$$\begin{aligned}
g_{f_c Q}^{(3)} &= g_{Q f_c}^{(3)} \\
&= -\frac{Q (2 Q \cos(\phi_0) - \sin(\phi_0))^2}{f_c (4 Q^2 + 1) (4 Q^2 + 2 Q \sin(2 \phi_0) + 1 + \cos(2 \phi_0))}, \\
g_{Q Q}^{(3)} &= \frac{(4 Q^2 + 1)^2 + (12 Q^2 - 1) \cos(2 \phi_0) + 2 Q (4 Q^2 - 3) \sin(2 \phi_0)}{2 (4 Q^2 + 1)^2 (4 Q^2 + 2 Q \sin(2 \phi_0) + 1 + \cos(2 \phi_0))},
\end{aligned} \tag{2.24}$$

where we have assumed $f_{\max} \gg f_c$ and retained only the leading terms in f_{\max}/f_c . Note that f_{\max} appears only in the component $g_{t_0 t_0}^{(3)}$ in this limit. In the next subsection, we shall argue that the dependence on f_{\max} will disappear from the final result if the maximization over t_0 is done with accuracy $dt_0 \lesssim 1/f_{\max}$.

The inequality $C(\phi_0; df_c, dQ, dt_0) \leq 1$ means that there will be a loss of SNR unless the actual parameters of a gravitational wave signal fall exactly onto one of the templates. In order to keep the detection efficiency high enough, we have to choose the template spacing so that the maximum value of the distance function is kept as small as possible.

C. Projection to 2-dimensional template space

The 3-dimensional metric on the template space $\{t_0, f_c, Q\}$ has a simple f_{\max} dependence in the large f_{\max} limit, namely, $g_{t_0 t_0}^{(3)} \propto f_{\max}$ and the other components are independent of f_{\max} . This fact allows us to reduce the problem of template spacing to that in the 2-dimensional space $\{f_c, Q\}$.

To reduce the 3-dimensional template space to 2-dimensions, let us note the distance function $ds_{(3)}^2$ may be rewritten as [23]

$$ds_{(3)}^2 = g_{t_0 t_0}^{(3)} \left(dt_0 + \frac{g_{t_0 I}^{(3)}}{g_{t_0 t_0}^{(3)}} dx^I \right)^2 + g_{IJ} dx^I dx^J, \tag{2.25}$$

where $\{x^I\} = \{f_c, Q\}$ and

$$g_{IJ} = g_{IJ}^{(3)} - \frac{g_{t_0 I}^{(3)} g_{t_0 J}^{(3)}}{g_{t_0 t_0}^{(3)}}. \tag{2.26}$$

We see that we can minimize the distance function (maximize the match) with respect to t_0 by filtering a data stream with respect to t_0 with accuracy $dt_0 = O(1/f_{\max})$, because we then have

$$g_{t_0 t_0}^{(3)} \left(dt_0 + \frac{g_{t_0 I}^{(3)}}{g_{t_0 t_0}^{(3)}} dx^I \right)^2 = O(f_c/f_{\max}) \rightarrow 0, \tag{2.27}$$

in the limit $f_{\max}/f_c \gg 1$. Thus, provided the matched filtering is done with this accuracy, which is normally practiced when we sweep over a data stream in time sequence, we may focus on the 2-dimensional space $\{f_c, Q\}$ for the problem of template spacing. Note that in the limit $f_{\max}/f_c \rightarrow \infty$, the reduced 2-dimensional distance function is given by

$$ds_{(2)}^2 = g_{IJ} dx^I dx^J = g_{IJ}^{(3)} dx^I dx^J. \tag{2.28}$$

Thus the f_{\max} dependence disappears completely.

Before proceeding further, we note that the metric g_{IJ} has a simple central frequency dependence which may be removed by the coordinate transformation,

$$\begin{aligned}
dF &= \frac{df_c}{f_c}; \\
f_c &\rightarrow F = \ln(f_c/f_0), \\
F &\rightarrow f_c = f_0 e^F,
\end{aligned} \tag{2.29}$$

where f_0 is some fiducial frequency. This transformation gives

$$\begin{aligned}
ds_{(2)}^2 &= g_{FF} dF^2 + 2 g_{FQ} dF dQ + g_{QQ} dQ^2; \\
g_{FF} &= f_c^2 g_{f_c f_c}, \quad g_{FQ} = f_c g_{f_c Q}.
\end{aligned} \tag{2.30}$$

Now, to find an appropriate tiling of the 2-dimensional template space, we consider contours of a fixed maximum distance $ds_{(2)}^2 = ds_{\max}^2$. Note that the metric has the initial phase dependence. So, the contour varies as ϕ_0 is varied (over the range $0 \leq \phi_0 \leq \pi$). The contours for $ds_{\max}^2 = 0.02$ are plotted in Fig. 1 in the case of the quality factor $Q = 2$. The thick curve shows the contour with $\phi_0 = 0$ which we considered in [20]. We see that if we use the previous template spacing given there, the minimum match is not guaranteed for other values of the initial phase ϕ_0 . It is therefore necessary to remedy this drawback when tiling the template space.

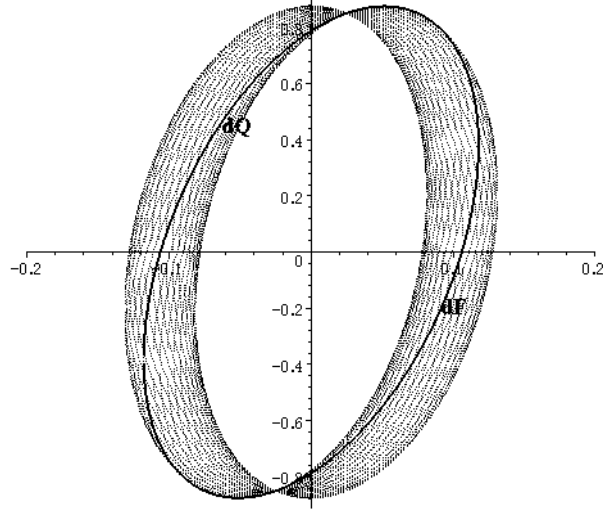


FIG. 1: Contours of the maximum distance $ds_{\max}^2 = 0.02$ for various initial phases. The quality factor is set to $Q = 2$. The thick curve shows the case of $\phi_0 = 0$, the interior of which corresponds to the region covered by one template in [20].

D. 2-dimensional template spacing

We now consider the template spacing that guarantees the minimum match for any value of ϕ_0 . As seen from Fig. 1, a conservative method is to take the interior of the inner envelope curve of the contours to be a region covered by each template. If we adopt such a template spacing based on the exact inner envelope curve, the computational cost of assigning grid points in the template space becomes high. We therefore choose to allow some redundancy, and construct an ellipse that can cover the interior of the inner envelope curve as much as possible. This also enables us to use the efficient method of template space tiling developed in [20].

Let us determine the inner envelope curve. It is convenient to perform a coordinate transformation that makes the envelope curve symmetric with respect to the axes of new coordinates. To do so, we first make a rotation in the (F, Q) -plane to bring the two points of intersection of all the contours on to the axes. This is achieved by the coordinate transformation

$$\begin{aligned} du &= \cos \theta dF + \sin \theta dQ, \\ dv &= -\sin \theta dF + \cos \theta dQ, \end{aligned} \quad (2.31)$$

where

$$\begin{aligned} \cos \theta &= \frac{1}{\sqrt{16Q^6 + 8Q^4 + Q^2 + 1}}, \\ \sin \theta &= \frac{Q(4Q^2 + 1)}{\sqrt{16Q^6 + 8Q^4 + Q^2 + 1}}. \end{aligned} \quad (2.32)$$

The metric components in the new coordinates are given by

$$ds_{(2)}^2 = g_{uu} du^2 + 2g_{uv} du dv + g_{vv} dv^2;$$

$$\begin{aligned}
g_{uu} &= \cos^2 \theta g_{FF} + 2 \cos \theta \sin \theta g_{FQ} + \sin^2 \theta g_{QQ}, \\
g_{uv} &= -\cos \theta \sin \theta g_{FF} + (\cos^2 \theta - \sin^2 \theta) g_{FQ} + \cos \theta \sin \theta g_{QQ}, \\
g_{vv} &= \sin^2 \theta g_{FF} - 2 \cos \theta \sin \theta g_{FQ} + \cos^2 \theta g_{QQ}.
\end{aligned} \tag{2.33}$$

Using the large Q expansion valid for $Q \geq 2$, the new coordinates u and v as functions of Q , to $O(1/Q^8)$ inclusive, are given by

$$\begin{aligned}
u &= \left[\frac{1}{4Q^3} - \frac{1}{16Q^5} + \frac{1}{64Q^7} \right] F + \left[Q + \frac{1}{160Q^5} - \frac{1}{448Q^7} \right], \\
v &= -\left[1 - \frac{1}{32Q^6} + \frac{1}{64Q^8} \right] F + \left[-\frac{1}{8Q^2} + \frac{1}{64Q^4} - \frac{1}{384Q^6} + \frac{3}{2048Q^8} \right].
\end{aligned} \tag{2.34}$$

The inverse transformation is given by

$$\begin{aligned}
F &= \left[-1 + \frac{1}{32u^6} - \frac{1}{64u^8} \right] v + \left[-\frac{1}{8u^2} + \frac{1}{64u^4} - \frac{1}{384u^6} + \frac{39}{10240u^8} \right], \\
Q &= -\frac{3}{16u^7} v^2 + \left[\frac{1}{4u^3} - \frac{1}{16u^5} + \frac{1}{64u^7} \right] v + \left[u + \frac{1}{40u^5} - \frac{17}{1792u^7} \right].
\end{aligned} \tag{2.35}$$

The contours of the maximum distance $ds_{\max}^2 = 0.02$ for $Q = 2$ on the (u, v) -plane are shown in Fig. 2.

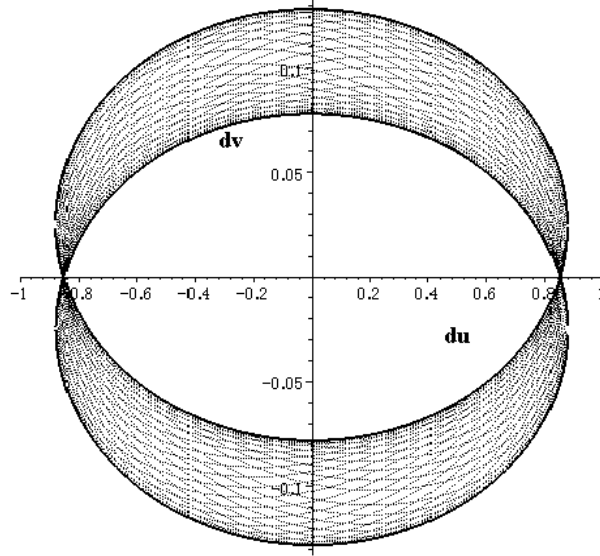


FIG. 2: Contours of the fixed maximum distance $ds_{\max}^2 = 0.02$ for $Q = 2$ on the (u, v) -plane with the metric (2.33).

Next, we derive the envelope curves. An envelope curve is the solution of the following two equations.

$$\begin{aligned}
R(du, dv; \phi_0) &= 0, \\
\frac{\partial}{\partial \phi_0} R(du, dv; \phi_0) &= 0,
\end{aligned} \tag{2.36}$$

where the function R is given in our situation by

$$R(du, dv; \phi_0) = g_{uu} du^2 + 2 g_{uv} du dv + g_{vv} dv^2 - ds_{\max}^2. \tag{2.37}$$

The envelope curve is obtained by eliminating the initial phase ϕ_0 from Eqs. (2.36). We find

$$\left[du + \frac{1}{Q(4Q^2 + 1)} dv \right]^2 = \frac{16Q^6 + 8Q^4 + Q^2 + 1}{4Q^5(4Q^2 + 1)^2}$$

$$\times \left[2Q(16Q^4 + 8Q^2 + 1)ds_{\max}^2 - Q(16Q^6 + 8Q^4 + Q^2 + 1)dv^2 \right. \\ \left. \pm (4Q^2 + 1)\sqrt{2(16Q^6 + 8Q^4 + Q^2 + 1)}ds_{\max}|dv| \right], \quad (2.38)$$

where Q is a function of u and v as given in Eq. (2.35). The outer and inner envelope curves are given by the plus and minus signs, respectively, in front of the square root in the above solution. Since our interest is in the inner envelope curve, we focus on the minus sign solution.

As we can see from Eq. (2.38), the envelope curve is still asymmetric with respect to both axes. To make it symmetric, we make a further coordinate transformation,

$$\begin{aligned} dV &= dv, \\ dU &= du + \frac{1}{Q(4Q^2 + 1)}dv, \end{aligned} \quad (2.39)$$

which gives the inner envelope curve in the form,

$$\begin{aligned} dU^2 &= \frac{16Q^6 + 8Q^4 + Q^2 + 1}{4Q^5(4Q^2 + 1)^2} \\ &\times \left[2Q(16Q^4 + 8Q^2 + 1)ds_{\max}^2 - Q(16Q^6 + 8Q^4 + Q^2 + 1)dV^2 \right. \\ &\quad \left. - (4Q^2 + 1)\sqrt{2(16Q^6 + 8Q^4 + Q^2 + 1)}ds_{\max}|dV| \right]. \end{aligned} \quad (2.40)$$

The equations (2.39) are integrated to give

$$\begin{aligned} V &= v \\ &= - \left[1 - \frac{1}{32Q^6} + \frac{1}{64Q^8} \right] F + \left[-\frac{1}{8Q^2} + \frac{1}{64Q^4} - \frac{1}{384Q^6} + \frac{3}{2048Q^8} \right], \\ U &= Q - \frac{1}{160Q^5} + \frac{1}{448Q^7}. \end{aligned} \quad (2.41)$$

The inverse transformation is given by

$$\begin{aligned} F &= \left[-1 - \frac{1}{32U^6} + \frac{1}{64U^8} \right] V + \left[-\frac{1}{8U^2} + \frac{1}{64U^4} - \frac{1}{384U^6} - \frac{9}{10240U^8} \right], \\ Q &= U + \frac{1}{160U^5} - \frac{1}{448U^7}. \end{aligned} \quad (2.42)$$

It is noted that the quality factor Q depends on only U . The inner and outer envelope curves are shown by the dotted curves in Fig. 3.

Finally, to use the efficient tiling method developed in [20], we look for an ellipse inside the inner envelope curve that can cover the region as much as possible. A simplest choice is to construct the ellipse tangent to the envelope curve at $dU = 0$ with the same curvature. This gives

$$\begin{aligned} ds_{\max}^2 &= \frac{2Q^4(\sqrt{4Q^2 + 1} + 1)}{\sqrt{4Q^2 + 1}(16Q^6 + 8Q^4 + Q^2 + 1)}dU^2 \\ &\quad + \frac{Q^2(16Q^6 + 8Q^4 + Q^2 + 1)}{(4Q^2 + 1)^2(2Q^2 + 1 - \sqrt{4Q^2 + 1})}dV^2 \\ &=: g_{UU}dU^2 + g_{VV}dV^2. \end{aligned} \quad (2.43)$$

This inner ellipse is shown by the thick curve in Fig. 3. It is noted that the ratio between the area covered by the inner ellipse and that by the inner envelope curve is 95.0% for $Q = 2$ and 99.4% for $Q = 20$, and this ratio is independent of the maximum distance ds_{\max} and the central frequency f_c .

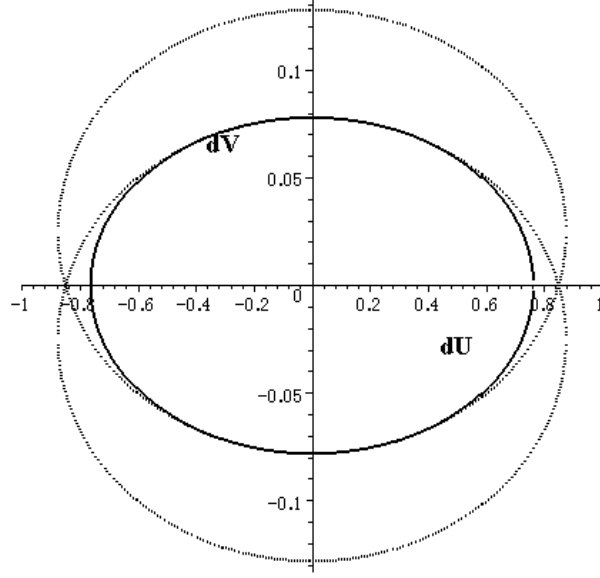


FIG. 3: The dotted curves show the inner and outer envelope curves for the maximum distance $ds_{\max}^2 = 0.02$. The thick curve is the ellipse given by Eq. (2.43). for all initial phases. Here we set $Q = 2$.

E. Conformally flat metric

Once we have an ellipse that ensures the minimum match we require, it is straightforward to apply our tiling method developed in [20]. To do so, we perform a coordinate transformation that transforms the 2-dimensional metric (2.43) to an explicitly conformally flat form. Namely, by the transformation,

$$\begin{aligned} dX &= -dV, \\ dY &= -\sqrt{\frac{g_{UU}}{g_{VV}}} dU, \end{aligned} \quad (2.44)$$

we obtain

$$ds_{\max}^2 = \Omega(Y) (dX^2 + dY^2), \quad (2.45)$$

where the conformal factor is given by

$$\Omega(Y) = g_{VV}(Q(Y)). \quad (2.46)$$

Up to $O(1/Q^8)$ inclusive, the coordinate transformation is explicitly given as

$$\begin{aligned} X &= \left[1 - \frac{1}{32Q^6} + \frac{1}{64Q^8} \right] F + \left[\frac{1}{8Q^2} - \frac{1}{64Q^4} + \frac{1}{384Q^6} - \frac{3}{2048Q^8} \right], \\ Y &= \frac{1}{2Q} - \frac{1}{16Q^2} - \frac{3}{64Q^3} + \frac{11}{1024Q^4} + \frac{31}{4096Q^5} - \frac{69}{32768Q^6} \\ &\quad - \frac{3357}{917504Q^7} + \frac{3891}{4194304Q^8} + \frac{248531}{150994944Q^9}. \end{aligned} \quad (2.47)$$

To the same accuracy, the inverse transformation becomes

$$\begin{aligned} F &= \left[1 + 2Y^6 + 3Y^7 + \frac{31}{8}Y^8 \right] X \\ &\quad + \left[-\frac{1}{2}Y^2 - \frac{1}{4}Y^3 - \frac{9}{32}Y^4 - \frac{1}{4}Y^5 - \frac{25}{96}Y^6 - \frac{17}{64}Y^7 - \frac{9447}{7168}Y^8 \right], \end{aligned}$$

$$Q = \frac{1}{2Y} - \frac{1}{8} - \frac{7}{32}Y - \frac{9}{128}Y^2 - \frac{31}{512}Y^3 - \frac{97}{2048}Y^4 - \frac{10649}{57344}Y^5 - \frac{7457}{32768}Y^6 - \frac{373751}{1179648}Y^7. \quad (2.48)$$

The conformal factor $\Omega(Y)$ is given by

$$\Omega(Y) = \frac{1}{8Y^2} + \frac{3}{16Y} + \frac{11}{128} + \frac{1}{128}Y - \frac{3}{2048}Y^2 + \frac{1}{4096}Y^3 + \frac{98297}{229376}Y^4 + \frac{303}{224}Y^5 + \frac{10661897}{4718592}Y^6. \quad (2.49)$$

When $Q = 2$, the errors induced by the above expansion are found to be $\sim 0.1\%$. This is accurate enough for our purpose as long as we allow the SNR loss, ds_{\max}^2 , of a few percent.

The fact that the conformal factor depends only on the coordinate Y is important. It allows us to apply the same tiling method developed in [20], which we recapitulate in Appendix A. In Fig. 8, we show the tiling of the template space in the (X, Y) coordinates. The tiling in the original coordinates (f_c, Q) is shown in Fig. 9.

III. TEST WITH TAMA NOISE SPECTRUM

The derivation of the template space metric (2.46) is based on the assumption that the noise is white. This assumption may be good because a ringdown wave will be rather narrow banded except for the case $Q \sim 2$. In order to confirm this, we examine the effectiveness of the tiling based on Eq. (2.46) in the case of a colored noise.

As a model of detector's noise, we use a fitting curve of the one sided noise power spectrum of TAMA300, which is given by

$$S_n(|f|) = \frac{3.0 \times 10}{f^8} + \frac{7.0 \times 10^{-16}}{f} + 7.0 \times 10^{-23} f^{1.2}, \quad (3.1)$$

where the frequency f is in units of Hz. This formula of the noise spectrum is obtained during Data Taking 8 in 2003 [24]. The normalization of the overall amplitude is arbitrary.

We prepare a template bank using Eq. (2.46). The minimum match is required to be 0.98. We also generate signals whose amplitudes are normalized to unity. Then, we perform the matched filtering and evaluate the maximum of the match for each signal. If the match is always greater than 0.98, the use of the template space metric (2.46) is justified even for a colored noise, at least for the TAMA DT8 noise spectrum.

Here we generated 2500 signals randomly with uniform probability in the range of the parameters $1.0 \times 10^2 \text{Hz} \leq f_c \leq 2.5 \times 10^3 \text{Hz}$, $2.0 \leq Q \leq 33.3$ and $0 \leq \phi_0 \leq \pi$. In Fig. 4, we plot the number of signals for each bin of the match. We see that the most of the signals are detected with the SNR loss less than 2%. Thus, the template spacing, constructed analytically under the assumption of the white noise, turns out to be valid even in the case of the colored TAMA noise spectrum.

IV. DISCUSSION

The detection of ringdown waves is a direct confirmation of the existence of a black hole. The ringdown waves have damped sinusoidal waveforms that reflect the mass and spin of a black hole. In our previous paper [20], we proposed an efficient method for tiling the templates for matched filtering in the 2-dimensional $\{f_c, Q\}$ space. However, it relied on the template space metric for signals with the initial phase $\phi_0 = 0$. In this paper, we took account of the initial phase dependence and developed a new, improved method to search for the ringdown waves.

Since the template metric depends on the initial phase, we first determined the inner envelope curve of all the contours of a fixed maximum distance ds_{\max}^2 between signals and templates on the (f_c, Q) -plane for all possible values of the initial phase. We then constructed an ellipse that can cover the region inside the inner envelope as much as possible. Finally, we applied our tiling method proposed in [20] to obtain an improved, reliable tiling of the template space.

Another change from our previous work is the difference in the definition of the match. In our previous work, we defined the match as the square of the SNR, ρ^2 , while here we used the SNR as the match. So, for the same fixed maximum distance, the number of templates needed to cover the template space turns out to be smaller than what we obtained previously, if we ignore the initial phase dependence. As a result, the actual number of templates to cover the template space did not increase much from what was suggested in [20].

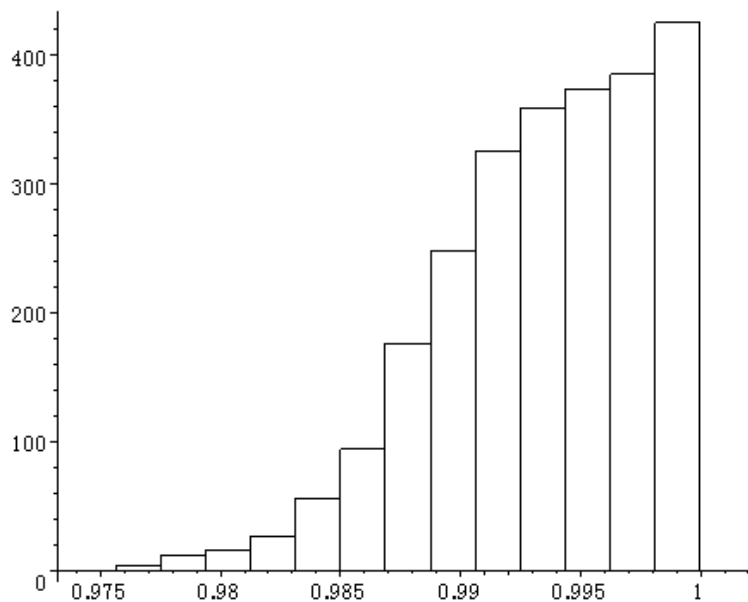


FIG. 4: The number of signals in terms of the value of the match between the signal and templates. The bank of templates are determined assuming the minimum match 0.98 using the metric (2.46) and the tiling method in [20]. The mean value of the match is 0.993.

We also examined the validity of our tiling method in the case of a colored noise spectrum by a Monte Carlo simulation. As a model of realistic noise power spectrum, we used a fitting curve of the noise power spectrum of TAMA300 during DT8 in 2003. For the pre-assigned maximum allowable SNR loss of 2%, we found that only a few out of 2500 signals had the SNR loss larger than 2%. This means that our template spacing is effective even in the case of colored noise.

Since the real data includes the non-stationary, non-Gaussian noise, it is necessary to check the effectiveness of this method in a realistic situation. Using the real data of TAMA300, this new template spacing is now being tested by Tsunesada et al. [25]. They find a lot of fake events due to the non-stationary, non-Gaussian noise. Particularly, the detector has many noise sources that can produce fake ringdown wave signals. Apparently, we need to develop a method to remove these fake events without losing real gravitational ringdown wave signals. Perhaps, the best way is to perform a coincidence analysis if we have plural detectors. We plan to study methods of coincidence or coherent analyses by using several detectors in the future.

Acknowledgments

We would like to thank N. Kanda and Y. Tsunesada for invaluable discussions and advice. We are also grateful to D. Tatsumi for useful comments. HN was supported by the Japan Society for the Promotion of Science for Young Scientists, No. 5919. This work was supported in part by the Grant-in-Aid for Scientific Research on Priority Areas (415) of the Ministry of Education, Culture, Sports, Science and Technology of Japan, and in part by Grant-in-Aid for Scientific Research Nos. 14047214 and 12640269.

APPENDIX A: EFFICIENT TILING METHOD

In Subsec. II E, we have derived the simple, conformally flat metric (2.45) for the template space. Here, using this metric, we formulate a tiling algorithm which is not only efficient but also quite simple.

1. Basis

To develop such a method, we note the following. Because of the conformal flatness, the contour of the fixed maximum distance $ds^2 = ds_{\max}^2$ centered at a point on the (X, Y) -plane is a circle for sufficiently small ds_{\max}^2 . Furthermore, along a line of $Y = \text{constant}$, $\Omega(Y)$ is constant. Thus, choosing first an appropriate $Y = \text{constant}$ line, say $Y = q_1$, we may place circles of the same radius with their centers located along the line $Y = q_1$ to cover a region surrounding that line. Then, if we find an algorithm to place circles along the $Y = q_1$ line and another algorithm to choose the next $Y = \text{constant}$ line, say $Y = q_2$, to be covered in an appropriate way, we can repeat this tiling procedure to cover the whole template space.

Let us assume that the template space to be tiled is a rectangle given by $F_{\min} \leq F \leq F_{\max}$ and $Q_{\min} \leq Q \leq Q_{\max}$. In the (X, Y) coordinates, this rectangle is mapped to the region bounded by the two $Y = \text{constant}$ lines corresponding to $Q = Q_{\min}$ and $Q = Q_{\max}$, which we denote by $Y = Y_0$ and Y_M , respectively, and the two lines $X = z_{\min}(Y)$ and $X = z_{\max}(Y)$ corresponding to $F = F_{\min}$ and $F = F_{\max}$, respectively. Note that $Y_0 > Y_M$ since large Y corresponds to small Q .

First, we construct a method to determine the spacing of the circles along each $Y = \text{constant}$ line. Let us consider the line $Y = q$ and place two circles with radius r centered at (p, q) and $(p + \Delta p, q)$,

$$(X - p)^2 + (Y - q)^2 = r^2, \quad (X - p - \Delta p)^2 + (Y - q)^2 = r^2. \quad (\text{A1})$$

We assume $\Delta p < 2r$ so that the two circles intersect at the two points, $(p + \Delta p/2, q \pm d(r; p))$, where $d(r; p)$ is the distance to each intersecting point from the line $Y = q$ (see Fig.5), given by

$$d(r; \Delta p) = \sqrt{r^2 - \frac{\Delta p^2}{4}}. \quad (\text{A2})$$

Our purpose is to tile the template space by the smallest possible number of filters. In order to do so, we choose the parameter p in such a way that the area defined by $S = \Delta p d(r; \Delta p)$ is maximized, i.e.,

$$\Delta p = \sqrt{2} r, \quad (\text{A3})$$

$$d = \frac{r}{\sqrt{2}}. \quad (\text{A4})$$

The radius r is determined by the value of ds_{\max}^2 and q as

$$r^2 = \frac{ds_{\max}^2}{\Omega(q)}. \quad (\text{A5})$$

In this way, we tile the region that covers the line $Y = q$.

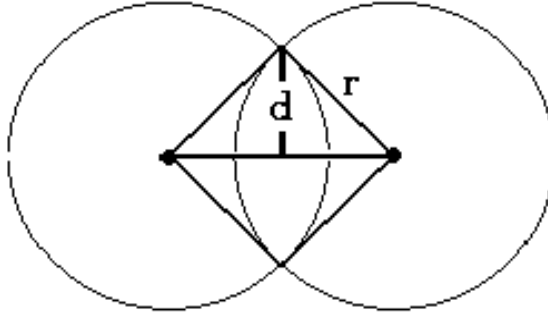


FIG. 5: Definition of d and r .

To choose the first line to be covered, we start from the point on the (X, Y) -plane corresponding to $(F, Q) = (F_{\max}, Q_{\min})$, that is, $(X, Y) = (X_0, Y_0)$ where $X_0 = z_{\max}(Y_0)$. Then we choose the first line $Y = q_1$ and the radius

r_1 so that the point (X_0, Y_0) is just on the edge of the first circle and an intersecting point of the first and second circles lies on the line $Y = Y_0$ as Fig. 6. This is achieved if the center of the first circle is at

$$(p_1, q_1) = \left(X_0 - r_1/\sqrt{2}, Y_0 - r_1/\sqrt{2} \right), \quad (\text{A6})$$

with the radius determined by solving Eq. (A5), which reads in the present case,

$$ds_{\max}^2 = r_1^2 \Omega(Y_0 - r_1/\sqrt{2}). \quad (\text{A7})$$

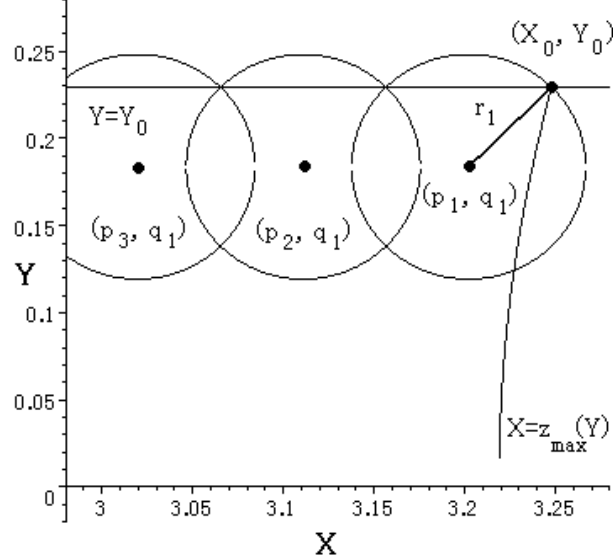


FIG. 6: Choosing the first line on the (X, Y) -plane.

Then the center of the n -th circle is at

$$(p_n, q_1) = \left(X_0 - (2n - 1) r_1/\sqrt{2}, Y_0 - r_1/\sqrt{2} \right), \quad (\text{A8})$$

and the number of circles needed to cover the line $Y = q_1$ is given by

$$N_1 = \left\lfloor \frac{L_1}{\sqrt{2} r_1} \right\rfloor, \quad (\text{A9})$$

where $[x]$ denotes the maximum integer smaller than $x + 1$ and L_1 is the coordinate length of X to be covered, i.e.,

$$\begin{aligned} L_1 &= z_{\max}(Y_0) - z_{\min}(Y_0) \\ &= F_{\max} - F_{\min} \\ &=: L. \end{aligned} \quad (\text{A10})$$

Once the covering of the first line is done, the second $Y = \text{constant}$ line is chosen as follows. Let $Y_1 = Y_0 - \sqrt{2} r_1$ and let (X_1, Y_1) be the intersecting point of the lines $Y = Y_1$ and $X = z_{\max}(Y)$, i.e., $(X_1, Y_1) = (z_{\max}(Y_1), Y_1)$. We choose this point as the starting point for the covering of the second line as Fig. 7. That is, the center of the first circle (p_2, q_2) on the second line $Y = q_2$ is

$$(p_2, q_2) = \left(X_1 - r_2/\sqrt{2}, Y_1 - r_2/\sqrt{2} \right), \quad (\text{A11})$$

with the radius r_2 determined again by Eq. (A5). Then the second line is covered by the same procedure we took for the first line. We repeat this procedure until we tile the whole template space we need to cover.

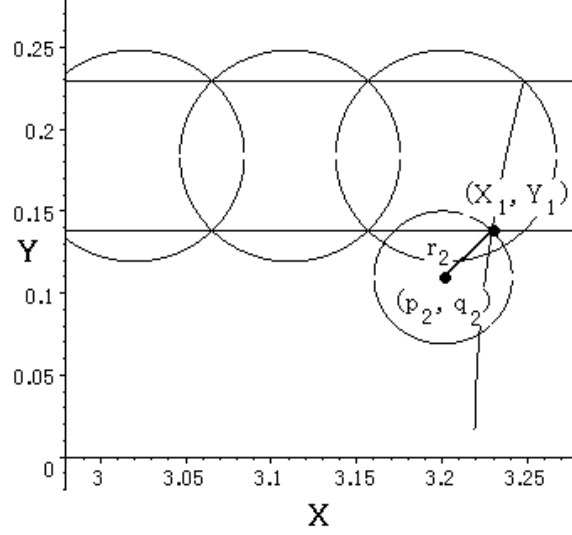


FIG. 7: Covering of the second line.

With this tiling procedure, the total number of templates is given as follows. Generalizing Eq. (A9), the number of templates for the i -th $Y = \text{constant}$ line ($Y = q_i$) is

$$N_i = \left\lceil \frac{L}{\sqrt{2} r_i} \right\rceil, \quad (\text{A12})$$

where r_i is determined by

$$ds_{\max}^2 = r_i^2 \Omega(Y_{i-1} - r_i/\sqrt{2}). \quad (\text{A13})$$

The number of $Y = \text{constant}$ lines necessary to cover the template space is determined by the minimum integer ν that satisfies the inequality,

$$\sum_{i=1}^{\nu} \sqrt{2} r_i \geq Y_0 - Y_M. \quad (\text{A14})$$

And the total number of templates is

$$\mathcal{N} = \sum_{i=1}^{\nu} N_i. \quad (\text{A15})$$

2. Application

Let us apply the method developed in the previous subsection to the case of the parameter space (f_c, Q) which has the range,

$$\begin{aligned} 1. \times 10^2 \text{Hz} &\leq f_c \leq 2.5 \times 10^3 \text{Hz}, \\ 2.0 &\leq Q \leq 20.0. \end{aligned} \quad (\text{A16})$$

We set $ds_{\max}^2 = 0.02$. This choice is made in order to make the SNR loss to be $\sim 3\%$ in the presence of colored noise as discussed in Sec. III. Using Eq.(2.29), we set $F = \ln(f_c/100\text{Hz})$. The above range corresponds to

$$\begin{aligned} 3.12 \times 10^{-4} &\leq X \leq 3.25, \\ 2.48 \times 10^{-2} &\leq Y \leq 2.29 \times 10^{-1}. \end{aligned} \quad (\text{A17})$$

| (f_c, Q) | (X, Y) |
|-----------------------------------|--|
| $1.0 \times 10^2 \text{Hz}, 2.0$ | $3.030840555 \times 10^{-2}, 2.293688750 \times 10^{-1}$ |
| $1.0 \times 10^2 \text{Hz}, 20.0$ | $3.124023844 \times 10^{-4}, 2.483796010 \times 10^{-2}$ |
| $1.0 \times 10^3 \text{Hz}, 2.0$ | $2.331909728, 2.293688750 \times 10^{-1}$ |
| $1.0 \times 10^3 \text{Hz}, 20.0$ | $2.302897494, 2.483796010 \times 10^{-2}$ |
| $2.5 \times 10^3 \text{Hz}, 2.0$ | $3.247808978, 2.293688750 \times 10^{-1}$ |
| $2.5 \times 10^3 \text{Hz}, 20.0$ | $3.219188225, 2.483796010 \times 10^{-2}$ |

TABLE I: The relation between the two coordinates (f_c, Q) and (X, Y) .

in the (X, Y) -space. (See Table I.)

Following the procedure described in the previous subsection, we choose the starting point (X_0, Y_0) which corresponds to $(f_c, Q) = (2.5 \times 10^3 \text{Hz}, 2.0)$. The radius r_1 is determined by Eq. (A7), or

$$0.02 = r_1^2 \Omega(Y_0 - r_1/\sqrt{2}). \quad (\text{A18})$$

Then all the parameters for our tiling method are determined. In Table II, we summarize the tiling parameters.

| i | (p_i, q_i) | (X_i, Y_i) | r_i | N_i |
|-----|---|---|------------------------------|-------|
| 0 | | $3.247808978, 2.293688750 \times 10^{-1}$ | | |
| 1 | $3.202211769, 1.837716656 \times 10^{-1}$ | $3.229142859, 1.381744561 \times 10^{-1}$ | $6.448419198 \times 10^{-2}$ | 36 |
| 2 | $3.200527260, 1.095588566 \times 10^{-1}$ | $3.222295278, 8.094325710 \times 10^{-2}$ | $4.046856890 \times 10^{-2}$ | 57 |
| 3 | $3.205093210, 6.374118861 \times 10^{-2}$ | $3.219985276, 4.653912012 \times 10^{-2}$ | $2.432739855 \times 10^{-2}$ | 94 |
| 4 | $3.209939255, 3.649309938 \times 10^{-2}$ | $3.219230312, 2.644707864 \times 10^{-2}$ | $1.420721877 \times 10^{-2}$ | 161 |
| 5 | $3.213469023, 2.068578968 \times 10^{-2}$ | | $8.147692989 \times 10^{-3}$ | 280 |

TABLE II: The parameters for the tiling of the template space are summarized. (X_i, Y_i) denotes the starting point of the i -th template spacing along the line $y = q_i$. (p_i, q_i) denotes the center of the first circle along the i -th line $y = q_i$, r_i is the radius of the circle, and N_i is the number of circles necessary to cover the i -th line.

It is noted that the number ν of the $Y = \text{constant}$ lines is very small,

$$\nu = 5. \quad (\text{A19})$$

The total number of templates is calculated to be $\mathcal{N} = 628$ ($\mathcal{N} = 1121$ for $Q_{\text{max}} = 59.4$). In Table III, we summarize the total number of templates \mathcal{N} with the range of the quality factor between $Q_{\text{min}} = 2.0$ corresponding to $a = 0$ and various maximum $Q_{\text{max}}^{(i)}$. Here i means the number of $Y = \text{constant}$ lines necessary to cover the template space, and the maximum quality factor is determined by this number.

In Fig. 8, we show the tiling of the template space in the (X, Y) coordinates. The tiling of the template space in the original coordinates (f_c, Q) is shown in Fig. 9.

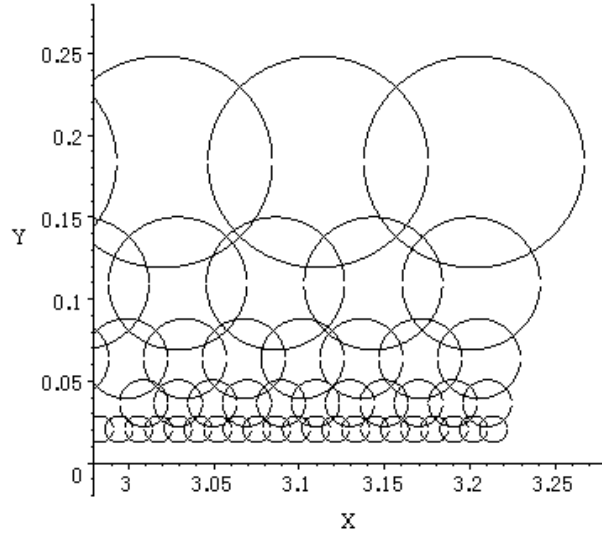
APPENDIX B: PARAMETER ESTIMATION ERRORS

Here we summarize the method to calculate the parameter estimation errors for gravitational ringdown waves. As a signal, we use the ringdown waveforms in Eq. (2.13) with the amplitude A ,

$$H(A, f_c, Q, t_0, \phi_0; f) = A \hat{h}(\phi_0; f_c, Q, t_0; f), \quad (\text{B1})$$

| i | $Q_{\max}^{(i)}(a)$ | \mathcal{N} |
|-----|----------------------------|---------------|
| 1 | 3.461857533 (0.7045454540) | 36 |
| 2 | 6.033964925 (0.9140427132) | 93 |
| 3 | 10.60831054 (0.9754675053) | 187 |
| 4 | 18.77484416 (0.9931010039) | 348 |
| 5 | 33.37367768 (0.9980786204) | 628 |
| 6 | 59.48251985 (0.9994680533) | 1121 |
| 7 | 106.1826585 (0.9998532378) | 1995 |

TABLE III: The maximum range of the quality factor and the number of templates.

FIG. 8: A part of the tiling of the template space in the (X, Y) coordinates. Templates are taken at the centers of the circles.

and the following calculation is done in the frequency domain. The parameter estimation errors are calculated by using Fisher information matrix

$$\Gamma_{\mu\nu} = (H_{,\mu}(A, f_c, Q, t_0, \phi_0), H_{,\nu}(A, f_c, Q, t_0, \phi_0)) , \quad (\text{B2})$$

where μ and ν are $\{\ln A, t_0, \phi_0, f_c, Q\}$. In practice, we consider $t_0 \rightarrow f_0 t_0$ and $f_c \rightarrow f_c/f_0$ with some frequency f_0 in the computational calculation. The root-mean-square errors σ_μ of parameters are obtained by

$$\sigma_\mu = \sqrt{\Sigma^{\mu\mu}} , \quad (\text{B3})$$

where $\Sigma = \Gamma^{-1}$, and the parameter correlation coefficients $c^{\mu\nu}$ between two parameters are

$$c^{\mu\nu} = \frac{\Sigma^{\mu\nu}}{\sqrt{\Sigma^{\mu\mu}\Sigma^{\nu\nu}}} . \quad (\text{B4})$$

In order to derive the Fisher information matrix, first we calculate $H_{,\mu}$ formally as

$$H_{,\ln A}(A, f_c, Q, t_0, \phi_0; t) = A \frac{1}{\sqrt{N(\phi_0; f_c, Q, t_0)}} \tilde{h}(f_c, Q, t_0, \phi_0; f) ,$$

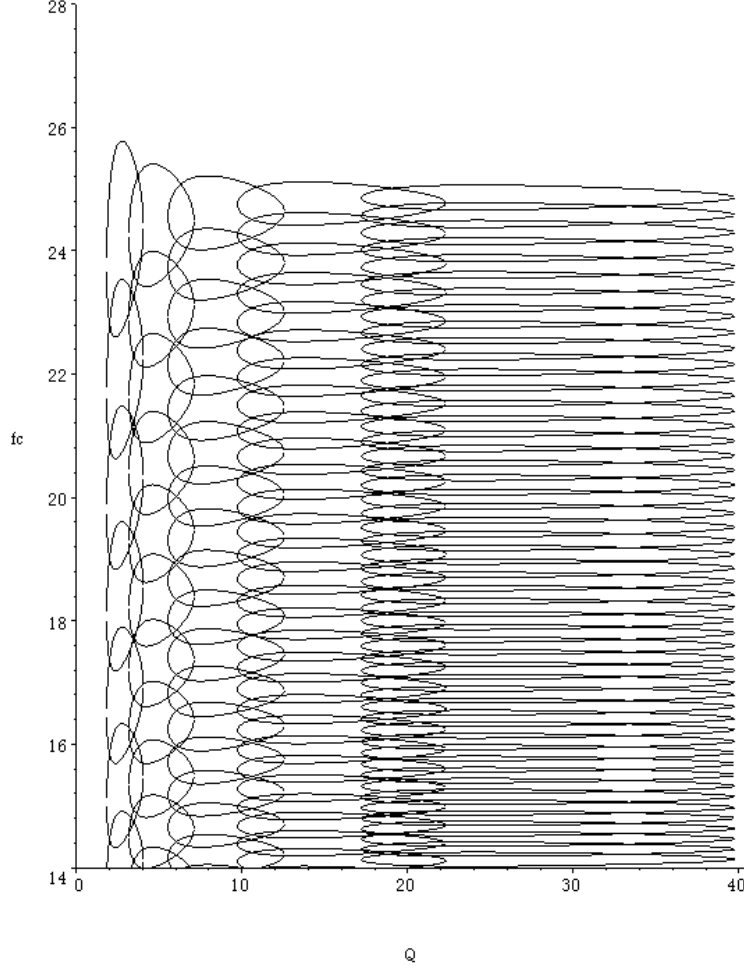


FIG. 9: A part of the tiling of the template space in the original coordinates (f_c, Q) with f_c measured in units of 100Hz. Note that the contour of $ds_{\max}^2 = 0.02$ for each template is warped.

$$\begin{aligned}
 H_{,t_0}(A, f_c, Q, t_0, \phi_0; t) &= A \frac{1}{\sqrt{N(\phi_0; f_c, Q, t_0)}} \tilde{h}_{,t_0}(f_c, Q, t_0, \phi_0; f), \\
 H_{,\alpha}(A, f_c, Q, t_0, \phi_0; t) &= A \left[-\frac{1}{N(\phi_0; f_c, Q, t_0)^{3/2}} (\tilde{h}_{,\alpha}(f_c, Q, t_0, \phi_0), \tilde{h}(f_c, Q, t_0, \phi_0)) \tilde{h}(f_c, Q, t_0, \phi_0; f) \right. \\
 &\quad \left. + \frac{1}{\sqrt{N(\phi_0; f_c, Q, t_0)}} \tilde{h}_{,\alpha}(f_c, Q, t_0, \phi_0; f) \right], \tag{B5}
 \end{aligned}$$

where α, β, \dots denote $\{\phi_0, f_c, Q\}$, and we have noted that the normalization constant N does not depend on the initial time. And then, the Fisher information matrix is given by

$$\begin{aligned}
 \Gamma_{\ln A \mu} &= A^2 \delta_{\ln A \mu}, \\
 \Gamma_{t_0 W} &= A^2 \frac{1}{N(\phi_0; f_c, Q, t_0)} (\tilde{h}_{,t_0}(f_c, Q, t_0, \phi_0), \tilde{h}_{,W}(f_c, Q, t_0, \phi_0)), \\
 \Gamma_{\alpha \beta} &= A^2 \left[-\frac{1}{N(\phi_0; f_c, Q, t_0)^2} (\tilde{h}_{,\alpha}(f_c, Q, t_0, \phi_0), \tilde{h}(f_c, Q, t_0, \phi_0)) (\tilde{h}_{,\beta}(f_c, Q, t_0, \phi_0), \tilde{h}(f_c, Q, t_0, \phi_0)) \right. \\
 &\quad \left. + \frac{1}{N(\phi_0; f_c, Q, t_0)} (\tilde{h}_{,\alpha}, \tilde{h}_{,\beta}) \right], \tag{B6}
 \end{aligned}$$

where $W = \{t_0, \phi_0, f_c, Q\}$.

Next, we may prepare the partial differentiation $\tilde{h}_{,W}$ of the ringdown waveforms to calculate the above Fisher

information matrix.

$$\begin{aligned}
\tilde{h}(f_c, Q, t_0, \phi_0; f) &= \frac{(\cos \phi_0 f_c - 2i \cos \phi_0 f Q + 2f_c Q \sin \phi_0) Q e^{2i\pi f t_0}}{\pi (2f_c Q - i f_c - 2f Q) (2f_c Q + i f_c + 2f Q)}, \\
\tilde{h}_{,t_0}(f_c, Q, t_0, \phi_0; f) &= 2i\pi f \tilde{h}(f_c, Q, t_0, \phi_0; f), \\
\tilde{h}_{,\phi_0}(f_c, Q, t_0, \phi_0; f) &= \frac{2f_c Q \cos \phi_0 - (f_c - 2if Q) \sin \phi_0}{2f_c Q \sin \phi_0 + (f_c - 2if Q) \cos \phi_0} \tilde{h}(f_c, Q, t_0, \phi_0; f), \\
\tilde{h}_{,f_c}(f_c, Q, t_0, \phi_0; f) &= \left[(16if f_c Q^3 - 4(f_c^2 - f^2) Q^2 + 4if f_c Q - f_c^2) \cos \phi_0 \right. \\
&\quad \left. - 2Q(4(f_c^2 + f^2) Q^2 + f_c^2) \sin \phi_0 \right] \tilde{h}(f_c, Q, t_0, \phi_0; f) \\
&\quad / \left[(2(f_c + f) Q + i f_c) (2(f_c - f) Q - i f_c) \right. \\
&\quad \left. \times ((f_c - 2if Q) \cos \phi_0 + 2f_c Q \sin \phi_0) \right], \\
\tilde{h}_{,Q}(f_c, Q, t_0, \phi_0; f) &= \left[f_c((2(f_c + f) Q + i f_c) (2(f_c - f) Q - i f_c) \cos \phi_0 \right. \\
&\quad \left. - 4i(f_c - 2if Q) f_c Q \sin \phi_0) \right] \tilde{h}(f_c, Q, t_0, \phi_0; f) \\
&\quad / \left[(2(f_c + f) Q + i f_c) (2(f_c - f) Q - i f_c) \right. \\
&\quad \left. \times ((f_c - 2if Q) \cos \phi_0 + 2f_c Q \sin \phi_0) Q \right]. \tag{B7}
\end{aligned}$$

In practice, by using the inner product (2.7) between two functions, we can obtain the root-mean-square errors and correlation coefficients of parameters.

-
- [1] LIGO web page: <http://www.ligo.caltech.edu/>
 - [2] VIRGO web page: <http://www.virgo.infn.it/>
 - [3] GEO600 web page: <http://www.geo600.uni-hannover.de/>
 - [4] R. J. Sandeman, in Second Workshop on Gravitational Wave Data Analysis, eds. M. Davier, and P. Hello, Editions Frontieres, Paris (1998).
 - [5] TAMA300 web page: <http://tamago.mtk.nao.ac.jp/>
 - [6] K. Kuroda *et al.*, Int. J of Mod. Phys. D **8**, 557 (1999)
 - [7] P. Astone *et al.*, Phys. Rev. D **47**, 362 (1993).
 - [8] E. Mauceli *et al.*, Phys. Rev. D **54**, 1264 (1996).
 - [9] D. G. Blair *et al.*, Phys. Rev. Lett. **74**, 1908 (1995).
 - [10] P. Astone *et al.*, Astroparticle Physics, **7**, 231 (1997).
 - [11] M. Cerdonio *et al.*, Class. Quant. Grav. **14**, 1491 (1997).
 - [12] LISA web page: <http://lisa.jpl.nasa.gov/>
 - [13] N. Seto, S. Kawamura and T. Nakamura, Phys. Rev. Lett. **87**, 221103 (2001).
 - [14] E. W. Leaver, Proc. R. Soc. Lond. A **402**, 285 (1985) and J. Math. Phys. **27**, 1238 (1986).
 - [15] F. Echeverria, Phys. Rev. D **40**, 3194 (1989).
 - [16] L. S. Finn, Phys. Rev. D **46**, 5236 (1992).
 - [17] E. E. Flanagan and S. A. Hughes, Phys. Rev. D **57**, 4535 (1998) and Phys. Rev. D **57**, 4566 (1998).
 - [18] J. D. E. Creighton, Phys. Rev. D **60**, 022001 (1999).
 - [19] N. Arnaud *et al.*, Phys. Rev. D **67**, 102003 (2003).
 - [20] H. Nakano *et al.*, Phys. Rev. D **68**, 102003 (2003).
 - [21] Y. Tsunesada and N. Kanda, unpublished work in progress.
 - [22] S. D. Mohanty, Phys. Rev. D **57**, 630 (1998).
 - [23] B. J. Owen, Phys. Rev. D **53**, 6749 (1996).
 - [24] D. Tatsumi, private communication.
 - [25] Y. Tsunesada *et al.*, in preparation.